Indian Journal of Engineering & Materials Sciences
Vol. 22, October 2015, pp. 487-496

Experimental and numerical investigations of sheet metal circular bending

Viorel Paunoiu[a]*, Mamane Abdou Saadatou[b], Dumitru Nedelcu[c] & Mircea Octavian[a]

[a]Department of Manufacturing Engineering, "Dunărea de Jos" University of Galaţi, 800201, Romania

[b]Ecole Nationale Superieure des Mines de Douai, France

[c]Department of Machine Manufacturing Technology, Gheorghe Asachi Technical University of Iasi, Iasi 700050, Romania

Received 31 January 2015; accepted 21 August 2015

Even the sheet metal bending is one of the most common metal working operations, the springback phenomenon that occurs after bending is necessary to be evaluated for obtaining a quality product. The aim of this paper is to study the influence of the bending angle, the punch radius and the sheet metal thickness toward the springback using a new experimental device for springback evaluation. This new device for springback evaluation is based on the circular bending of sheet metal. Using FEM, a numerical study is made in order to certify the experimental values results of the springback obtained by applying the circular bending method. The results validate the new bending device which could be used as a tool for dimensional control in bending and for prediction the suitable process parameters in springback reduction.

Keywords: bending, circular bending, sheet metal forming, springback, simulation

Air bending is the most common type of bending used in sheet metal shops today. In this process the blank is deformed in a die along one axis under the punch pressure (Fig. 1). The blank is initially bent in an elastic region. As the process continues, the blank is deformed by plastic deformation, thereby changing its shape. In the bending process, the bending load increases until the elastic limit of the material is exceeded[1,2]. The material state enters the plastic deformation region and sheet metal can be formed. Specifically, the stress generated in the blank is greater than the yield strength but lower than the ultimate tensile strength of the material[3,4]. The blank initially deforms where the bending moment is the greatest.. During the bending operation, the outer surface of the work-piece generates the greatest stretch, which then propagates inward toward the neutral plane. Similarly, the inner surface of the work-piece generates the greatest compression, which also then propagates inward toward the neutral plane.

As the bending force is removed at the end of the bending stroke, the inner surface–generated compressive stress tries to enlarge the work-piece and the outer surface–generated tensile stress tries to shrink. In contrast, the elastic band remains in the bent parts trying to maintain its original shape, resulting in a partial recovery toward its initial shape[4]. This elastic recovery is called "spring-back" after air bending, dimensional change of the shape after releasing the tool due to elastic effects appears. This phenomenon is known as springback or elastic recovery (Fig. 2)[5].

Thus to obtain a sound part with a good dimensional accuracy and form it is necessary to known the level of this elastic recovery, which is dominating in bending, and also the factors which influence this process. The springback in air bending, is difficult to quantify, and in general, after the forming, the bend profile is measured and the tools are changed.

Several experimental and numerical studies have been devoted to the study of the springback phenomenon. The experimental researches aimed to develop methods to quantify the size of the springback. Thus, a tool which incorporated sensors to control the springback in L-bending was proposed by Ming *et al*.[6] A hydraulic press with active control for evaluating springback was proposed by Sun *et al*.[7] Ferreira *et al*.[8] developed a method which is using computer vision and digital image processing to automatically measure the springback angles.

The numerical simulation of bending is attractive to reduce the waste of time and cost with trials. Finite element method is the main numerical solution used to study the effect of different process parameters and validate analytical models in bending

*Corresponding author (E-mail:viorel.paunoiu@ugal.ro)

process[9]. Some springback reduction methods used in U-channel bending process with the FEM were analyzed by Chou and Hung[10]. The accuracy of forming stright ribs using silicone rubber by FEM was studied by Quadrini *et al.*[11] Esat *et al.*[12] analyzed the bending and springback of different aluminum materials with different thickness. Hama *et al.*[13] analyzed the springback in sheet metal forming using a new method for define the tool surface. Alfaidi[14] presents a review of techniques for determination the springback in sheet metal forming including FEM methods.

The above analysis shows that springback phenomenon includes a broad issue that opens wide possibilities for research. In this context the paper presents a new device for springback prediction based on circular bending. The device gives the possibility to deform and to measure the springback after forming without any supplementary tool. Also the device gives the possibility to springback reduction, by controlling the bending angle after deformation process. In comparison with the wipe bending, using circular bending, the friction is reduced and the risk of producing scratches, because the punch is moving over the sheet surface, is removed. The numerical simulation using FEM are made to complete the analysis of the circular bending method with the new device for springback prediction.

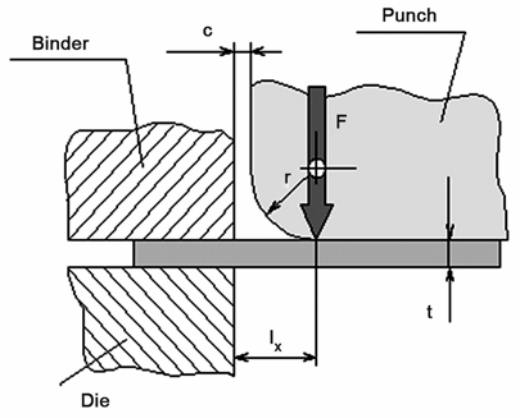

Fig. 1 – Wipe bending

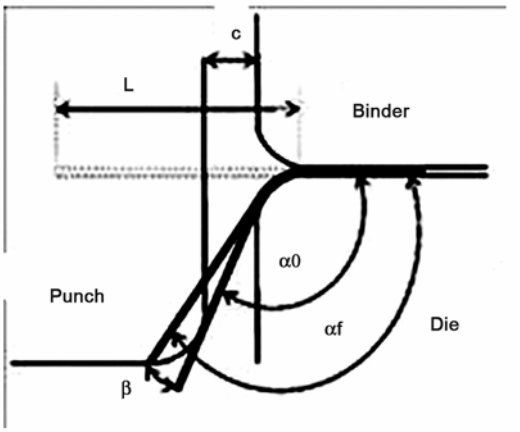

Fig. 2 – Springback in bending

Experimental Procedure

Experimental device for springback prediction in circular bending process

The circular bending method for springback prediction is presented in Figs 1-4. Both the method and the device are patented[15].

Figure 3 presents the initial position in circular bending. The sample 1 is clamped with the force *Q*, between the fixed punch 2 and the restraint plate 4. The rotating arm 3, with a roll as active element is in contact with the blank with the help of a metallic spring, which is not represented in figure. The rotating arm and the rotating disk are moving circular around the fixed point C. The rotating disk has marked on its surface four scales corresponding to

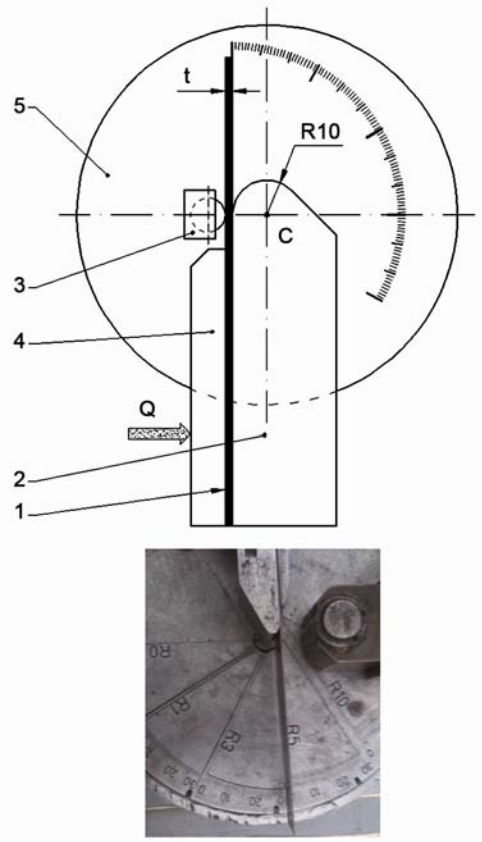

Fig. 3 – Device in initial position

the four punches of 1, 3, 5 and 10 mm bending radii respectively, and to the bending angles of 30°, 60°, 90°, 120° and could be rotated from 30° to 30°. After each rotation the disc is blocked with the help of an indexer, which is not presented in figures (see Fig. 7). In initial position the blank is aligned with the scale corresponding to the bending radius. Figure 4 presents an intermediate position, where the rotating arm are moving circular and deforms the material around the punch radius.

Figure 5 shows the final position of bending. Finally, in this position the rotating arm is retracted (Fig. 6), the material will springback, and on the scale it will be read the value of springback. The process will be resumed for the next measurement, by rotating the disk, for another angle and/or by changing the punch with another radius.

The device (Fig. 7) materializes the circular bending process presented above. The device uses samples with widths between 10-15 mm and thickness between 0.5-1.5 mm.

Figure 8 presents the images of punches. Figure 9 shows the image of the rotating disc as the main component of the device which gives the possibilities to measure the value of springback.

The sample 1 is fixed between the punch 2 using the restraint plate 4. A bending radius and a bending angle are established. The rotating disk 5 is moving circular till the sample is aligned with the scale of the bending radius. The blocking button 6 is released and the rotating arm 3 comes in contact with the sample. Then the rotating disk 5 is circular moved for obtaining the bending angle. The rotating arm will be manually actuated and will deform the sample in a circular moving. After bending to the target angle (marked on the rotating disc 5) the rotating arm is retracted and blocked and the material will springback. The bending angle and the springback angle are measured on the interior profile of the part. The springback angle will be read on the graded scale of the rotating disc 5. Using the rotating disc 5, the reading is simple and rapid with a good precision, the scale being divided with a step of 1°. The indexing system 10 is used for positioning the rotating disk 5 depending on the bending angle and radius. The punches 2 are exchangeable and their position is established within the guide 9.

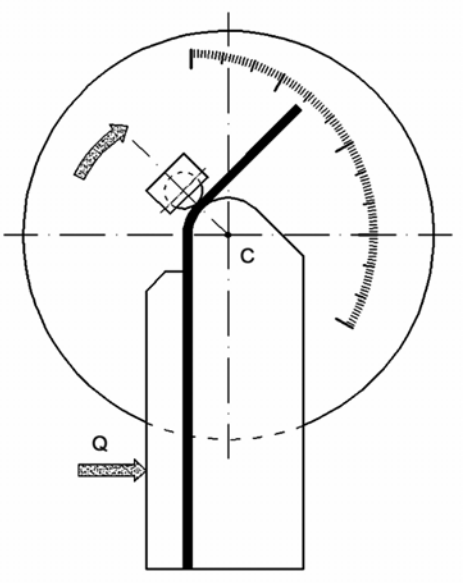

Fig. 4 – Device in intermediate position

Results and Discussion

Experimental results for circular bending process

In order to perform the experimental part of the study, steel sheets with different thicknesses were considered, details on material properties are shown

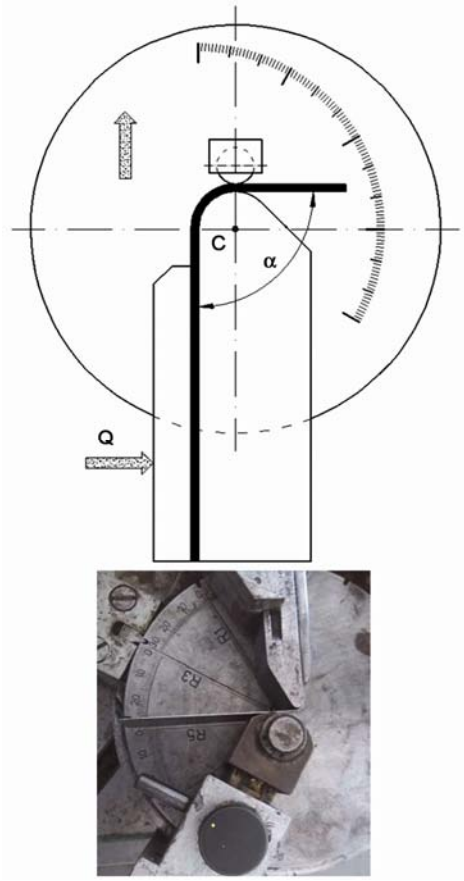

Fig. 5 – Device in final position

in Table 1. Rectangular shaped specimens of 200×15 mm were used. The tensile test specimens were cut according to ASTM E8/E8M-09 by using WJC to eliminate edge effect problems that are associated with mechanical shearing operations. A 100 kN tensile testing machine that has hydraulic wedge grips was used for all tests. A mechanical extensometer was used for elongation measurement. The cross head speed, v= 0.15 mm/s, were chosen for all tests since the materials are assumed to be not strain rate dependent at room temperature[20]. Three tensile specimens were pulled until they crack for each

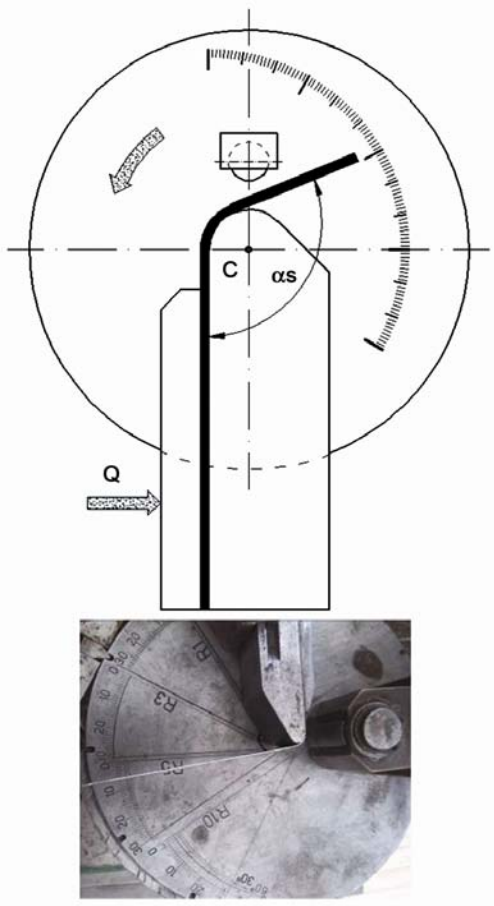

Fig. 6 – Device after springback

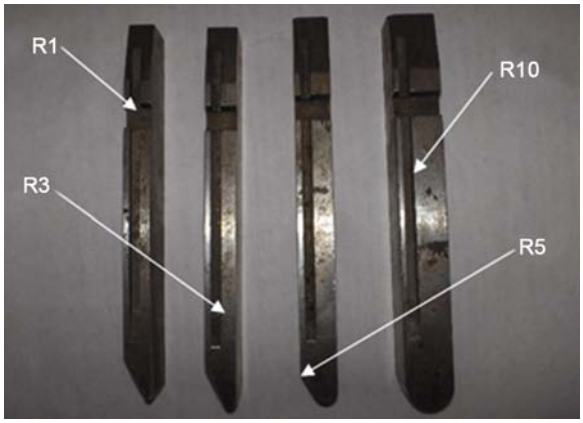

Fig. 8 – Punches

Fig. 9 – Rotating disk

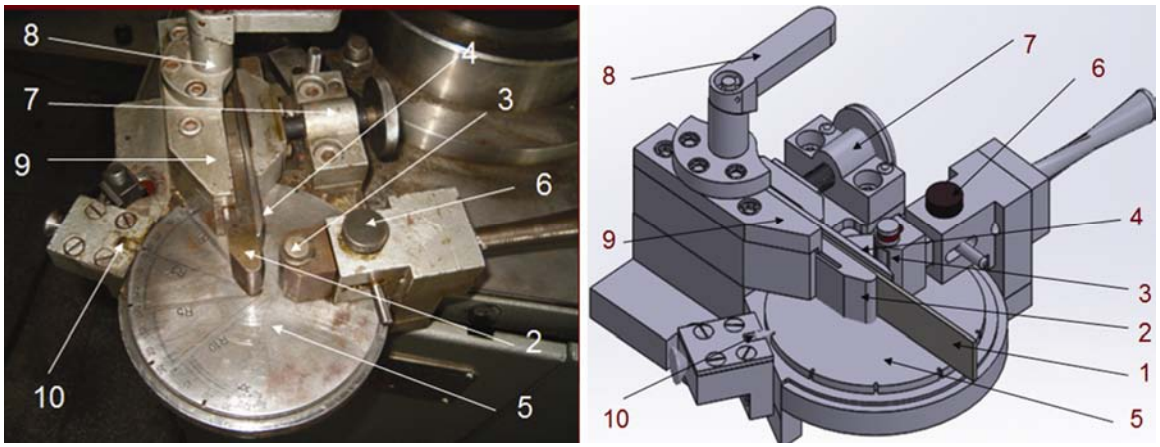

Fig. 7 – Device for springback dimensional control

Table 1 – Materials properties

Material	Thickness, mm	Yield strength ($Rp_{0,2}$),MPa	Tensile strength (R_m),MPa	Strain hardening exponent (n)	Anisotropy coefficient (r)	Strength coefficient (K), MPa
Steel Sheet Metal	0.8	209.6	336.0	0.194	1.348	461
	0.9	240.0	348.0	0.191	1.139	477
	1.2	215.0	326.0	0.165	2.011	438

direction (rolling, transverse and diagonal) to obtain flow curve. Load, stroke and engineering strain values, elastic modulus, yield strength, hardening exponent and anisotropy coefficients were obtained as output from the machine software. The measured values are gien in Table 1.

The relationship between true stress and true strain, i.e., the flow tress curve can be expressed using the power law as shown in Eq. (1):

$$\sigma = K\,\varepsilon^{n} \quad \ldots (1)$$

where K is the strength coefficient (Eq. (2) and Table 1), ε is the plastic strain, n is strain hardening exponent.

Given n and tensile strength R_m the user can solve for K as follows[16]:

$$K = \frac{R_m}{n^n} \quad \ldots (2)$$

Angle of springback $ß$ is given by:

$$\beta = \alpha_s - \alpha \quad \ldots (3)$$

Where α_s is the interior springback angle (°), α is interior bending angle (°).

Figures 10 and 11 present some images of the parts obtained using the device for circular bending method, after springback.

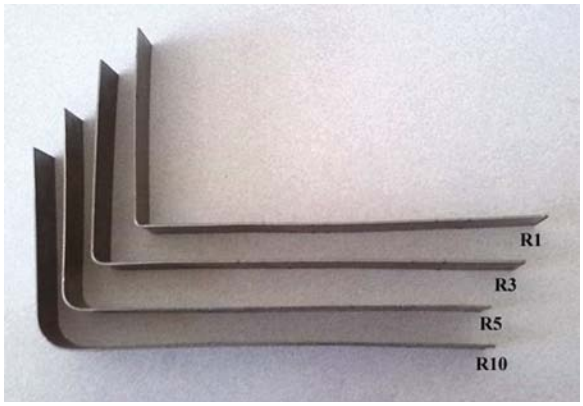

Fig. 10 – Circular bending at different radii, material thickness 1.2, bending angle 90°g

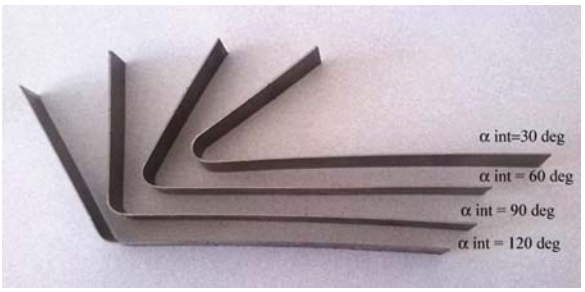

Fig. 11 – Circular bending at different angles, material thickness 1.2, punch radius 5 mm

Effect of punch radius and sheet thickness on springback

For investigation the effect of punch radius r_p and the sheet thickness toward the springback, the four punches with radius of 1, 3, 5 and 10 mm, respectively and three blanks with the thickness of 0.8, 0.9 and 1.2 mm, respectively were used. Considering the interior bending at 90° for all cases, the influences of the ratio punch radius/sheet thickness are shown in Fig. 12. The springback angle was measured on the interior profile of the part.

The curves show that springback increases when the ratio punch radius/sheet thickness increases, at the same material thickness. This makes sense because a bigger radius means that the stress in the material due to bending will be lower and therefore the ratio plastic deformation vs. elastic deformation will be smaller which leads to a greater springback[17,18].

Also, in our case, the springback decreases when the material thickness increases, at the same punch radius. According to Biradar and Deshpande[19] and Jiang *et al.*[20,] it is because the more thicker plate can bring larger surface stress, and more materials have undergone plastic deformation, thereby decreasing the springback.

Effect of interior bending angle and the sheet thickness on springback

For investigation the effect of bending angle and the sheet thickness toward the springback, the four bending angles 30°, 60°, 90° and 120°, respectively, and three blanks with the thickness

of 0.8, 0.9 and 1.2 mm, respectively, were considered. Using a punch radius r_p of 5 mm, for all cases, the influences of the bending angle and the sheet thickness are presented in Fig. 13. The bending angle and the springback angle were measured on the interior profile of the part.

Considering the interior angles, before and after deformation, the results show that the springback decreases when the interior bending angle increases regardless of the material thickness. This is because at a certain punch radius, the greater the interior bending angle the tensile and compressive stresses on the inner and outer surfaces are decreased, which leads to a decrease of the springback[21]. In addition, the stress along the section becomes more uniform as the thickness increases, which is also a reason for the decrease of the springback.

A coordinate measuring machine was used to validate the experimental results. The comparison between the measured values of springback on the device and on the CMM are given in Table 2.

The coordinate machine measured values are closer to the experiment values.

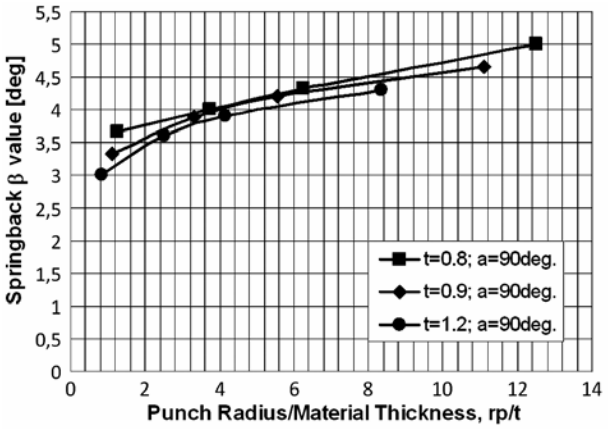

Fig. 12 – Springback values for different ratio punch radius/ material thickness

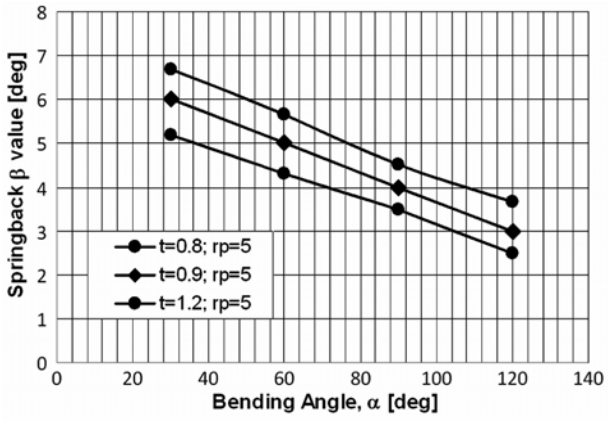

Fig. 13 – Springback values for different bending angles and sheet thickness

Numerical simulation of springback using circular bending process

Accurate springback prediction is essential for tool design and quality control in sheet forming processes. For springback evaluation using numerical simulation two stages are required to be completed the deformation stage and the springback evaluation stage. Explicit solvers can be used to simulate dynamic analysis and allow to evaluate large deformations (like in deep drawing), whereas implicit solvers are suitable to simulate static analysis (like the springback phenomenon)[22]. Thus, in metal forming process simulation of components, a final implicit static step may be used to obtain a static springback solution after the tool is removed from the die. In this way, the springback solution starts from the stress strain state of the forming simulation without numerical dynamic oscillations[22].

The springback is a sensitive process, which is not only influenced by springback computation itself, but also sturdily depends on the accuracy of previous forming simulation process. There are so many numerical parameters influencing the accuracy of spring back calculation, that it is not easy to obtain robust and accurate springback[21].

For the deformation stage was used the new Roller Hemming module from Dynaform 5.9 program. Hemming is a technology used by the automotive industry to join inner and outer closure panels together (hoods, doors, tailgates, etc.). It is the process of bending/folding the flange of the outer panel over the inner one. The geometric elements of the module are the outer panel, inner panel, roller, hem bed and the binder. For the roller, in Roller Hemming module, is defined a trajectory which assists the assembly process.

Table 2 – Springback measured values

Punch radius, mm	Bending angle, degree	Blank thickness, mm	Experimental springback, degree (CMM)	Experimental springback, degree (measured on the device)
5	30	1.2	4.99	5.2
	60	1.2	4.12	4.3
	90	1.2	3.31	3.5
	120	1.2	2.30	2.5

The module was adapted to the present situation and the geometric model is presented below:

In the present case, the outer panel is defined by the blank, the inner panel is not defined, the roller is the defined by the roll, the hem bed is the punch and the binder (Fig. 14).

Four different models with various punch radii 1, 3, 5 and 10 mm, respectively were designed. Figure 15 shows these cases. The trajectories of the roll around the punch radius which determine the bending process are also presented in the above figure.

The materials used in simulations are similar with those ones given in Table 1. The blank is a rectangular plate with the dimensions of 200×15 mm as in the experimental part. The roll has a diameter of 10 mm.

The tooling was modeled as rigid surfaces**.** The FE blank mesh consists of 4-node Belytschko-Tsay shell elements, with five integration points through the thickness of the sheet[11]. The Coulomb friction law was used with a friction coefficient of 0.125, which characterize the contact steel/steel[1]. This is the implicit value used in Dynaform progrm[16]. The roll speed around the punch was 50 rad/s. The binder force was of 2000 N. Five integration points were allocated along the thickness direction to take up the bending deformation.

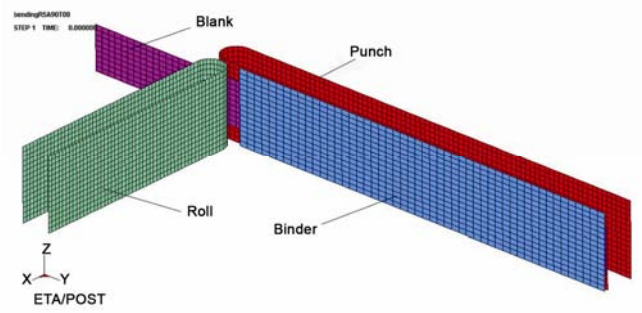

Fig. 14 – Geometrical model for numerical simulation

A special one-way forming contacts are recommended[20] with the work-piece defined on the slave side (contact forming one way surface to surface). Orientation is automatic with forming contacts. Forming contact tracks the nodal points of the blank as they move between the elements of the tooling surface. Penalty forces are used to limit penetrations. In the model the deformable blank formed the slave side and the rigid tools formed the master side interface in the contact definitions. Generally, this type of contact option is recommended since the penetration of master nodes through the slave surface is considered in adaptive remeshing. In adaptive remeshing the mesh of the blank refines to capture sharp details in the master surface, and the master surface will protrude through the blank[23].

Results of numerical simulations of springback using circular bending process

According with the experimental work, the simulation work followed the same analysis of the influence of the process parameters toward the springback values.

Figures 16-18 show the images of the bent parts, before and after sprinback, for the same punch radius, r_p=5 mm and for different bending angles and sheet thickness. The images from below must be read

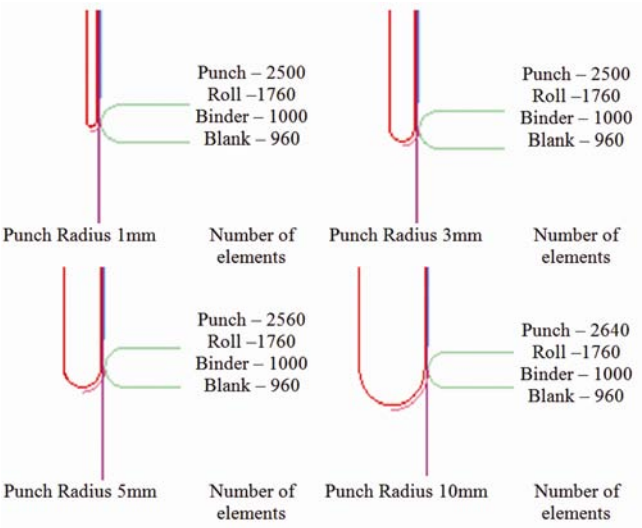

Fig. 15 – Details of the geometrical models and roll trajectories

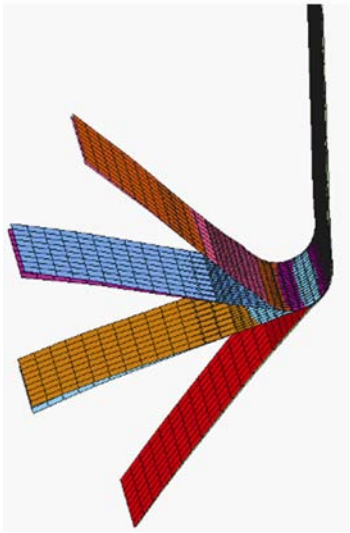

Fig. 16 – Bending simulation: t=0.8 mm, r_p 5 mm

according to the image from Fig. 12. Using this method an interior angle of 120° match with a bending angle of 60° and so on. As a result, for all cases, increasing the bending angle has as effect decreasing the springback.

Table 3 presents a comparison between the experimental and numerical results in circular bending. Most of the numerical values are close to the experimental values. For bending at the 30° the obtained numerical results are not satisfactory. A springforward appears which is not confirmed by the experimental results.

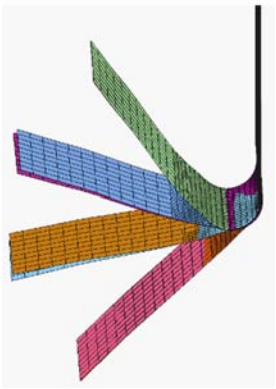

Fig. 17 – Bending simulation: t=0.9 mm, r_p 5 mm

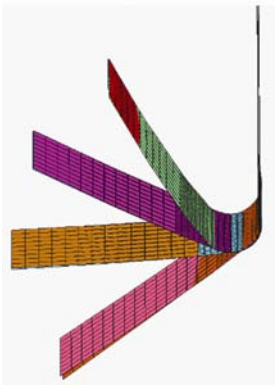

Fig. 18 – Bending simulation: t=1.2 mm, r_p 5 mm

Figures 19-22 present the qualitative distibution of σ_{xx} and σ_{yy} stresses, on the inner and outer layers, for the sheet thickness of 0.9, punch radius 5 mm and bending angle of 90°.

The inner and outer layers are in different states, that generates springback. Therefore, stresses are nonuniform, which produce the springback after that are uploaded.

Figures 23 and 24 present the qualitative distibution of max. Von Mises stress, after springback, for the sheet thickness of 0.8 and 0.9 mm, respectively.

The margins enter the plastic state while the middle remains in elastic state, having as a result the generatation of springback after offloading. As a result, the bending angle and the curvature radius are changed, which affects the final shape of the bending parts.

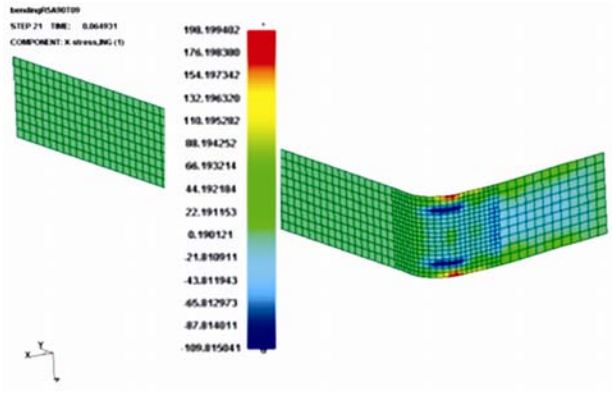

Fig. 19 – σ_{xx} stress at circular bending on inner layer

Tabel 3– Springback variation in circular bending

Punch radius (mm)	Bending angle (°)	Blank thickness (mm)	Experimental springback (°)	Numerical springback (°)
5	30	0.8	6.67	-
		0.9	6	-
		1.2	5.20	-
	60	0.8	5.67	5
		0.9	5	4.2
		1.2	4.3	3.9
	90	0.8	4.5	4
		0.9	4.0	3.5
		1.2	3.5	2.5
	120	0.8	3.67	2.9
		0.9	3	2
		1.2	2.50	2.6

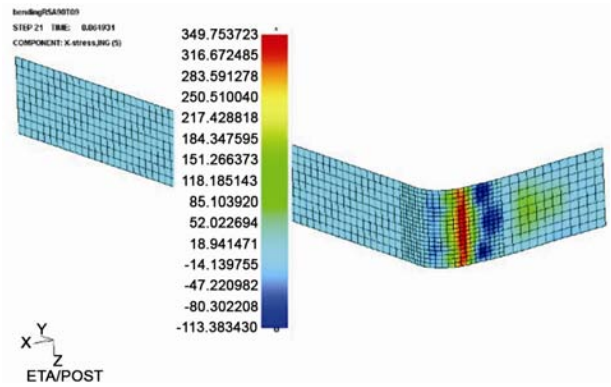

Fig. 20 – σ_{xx} stress at circular bending on outer layer

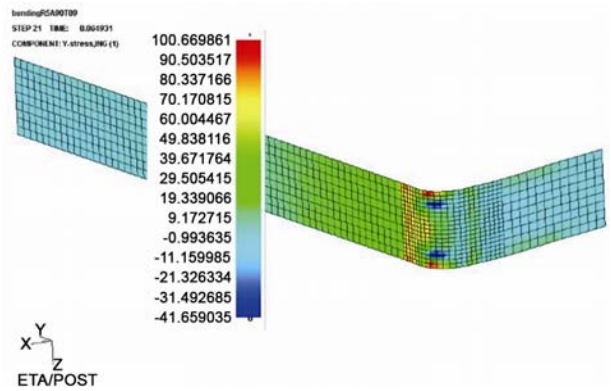

Fig. 21 – σ_{yy} stress at circular bending on inner layer

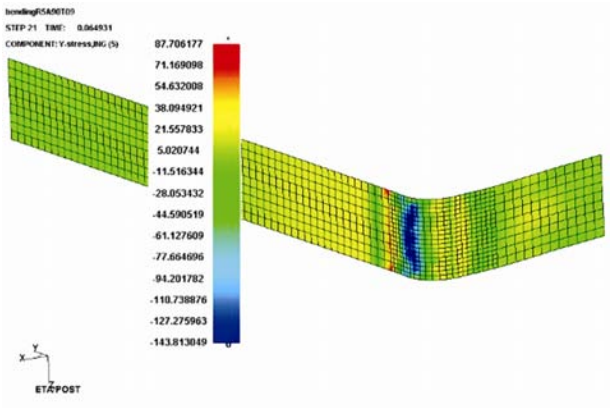

Fig. 22 – σ_{yy} stress at circular bending on inner layer

The values from the Fig. 25 are measured along the lenghts of samples, in the middle. The numerical values show values of max. Von Mises stresses after unloading. Curves have the same aspect and next zone could be indentified: one is the undeformed zone which correspond to the area of sample clamping, then is the elasto-plastic zone which match with the radius zone (bending zone) and the last zone is the

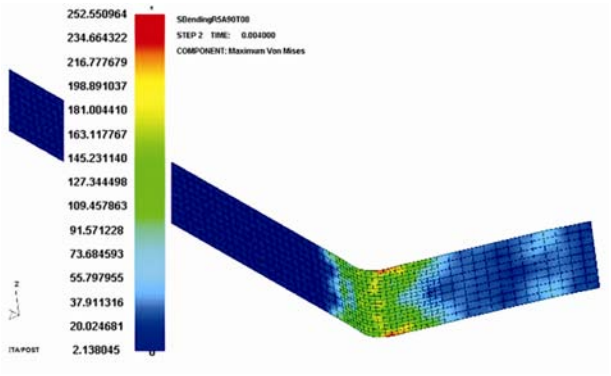

Fig. 23 – Max. Von Mises after springback at circular bending at 90°, material thickness 0.8 mm

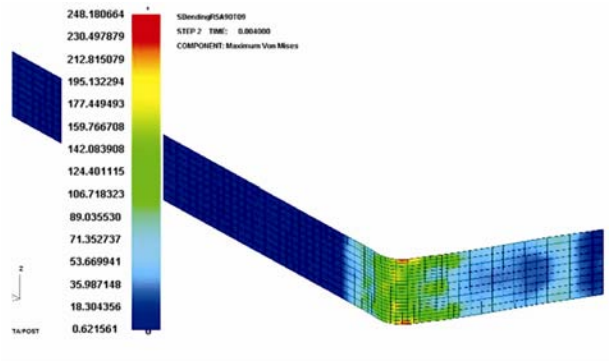

Fig. 24 – Max. Von Mises after springback at circular bending at 90°, material thickness 0.9 mm

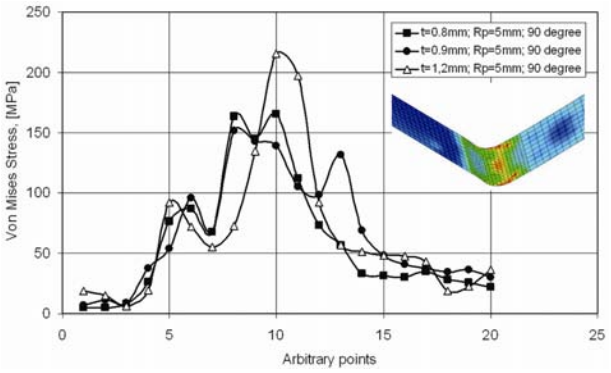

Fig. 25 – Max. Von Mises stresses after springback

elastic zone, which match with the free end of the sample. The last two zones according to Altan and Tekkay[2] are responsible for springback phenomenon.

Conclusions

The springback phenomenon in circular bending by experimental and numerical simulations considering a new device was studied. The following conclusions can be drawn from this study:

i) The device used in experiments assures, according to the bending parameters such as the punch radius and bending angle, in an appropriate mode, simply and rapidly the determination of springback. The device assures the study of the influence of the bending radius and bending angle toward the springback on samples with a width between 10-15 mm and thickness between 0.5-1.5 mm.

ii) The experimental works prove the validity of the results obtained using the device, the differences between the values measured on the samples with the device and using a CMM are negligible.

iii) The numerical simulations validate the experimental results in most of the studied cases. An important gain was the application of the Hemming Dynaform module to the circular bendings. The simulations certify that simulation parameters must be carefully and accurately set to obtain the expected results.

iv) The results come to validate the new device which could be used in an industrial context for establishing the bendenability of sheet metal and in research for quantify the process parameters in springback reduction.

References

1 Lange K, Ed, *Lehrbuch der Umformtechnik*, (Band 3: Blechumformung, Springer, Berlin), 1975.

2 Altan T & Tekkay A Erman, *Sheet Metal Forming: Processes and Applications*, (ASM International), 2012.

3 Banabic D, *Sheet Metal Forming Processes, Constitutive Modeling and Numerical Simulation*, (Springer), 2010.

4 Thipprakmas Sutasn, *Finite Element Analysis on V-Die Bending Process*, edited by Moratal David, 2010.

5 Gan W & Wagoner R H, *Int J Mech Sci*, 46 (2004) 1097-1113.

6 Ming Y, Manabe K, Nishimura H, *Smart Mater Struct*, 7(4) (1998) 530-536.

7 Sun P, Grácio J J, Ferreira J A, *J Mater Process Technol*, 176 (2006) 55-61.

8 Ferreira J A, Sun P, Grácio J J, *J Mater Process Technol*, 177 (2006) 377-381.

9 Reddy P V R Ravindra, Reddy G Chandra Mohan, Reddy T A Janardhan, *Indian J Eng Mater Sci*, 19 (2012) 24-30.

10 Chou I N & Hung C, *Int J MachTools Manuf*, 39(3) (1999) 517-536.

11 Quadrini F, Santo L, Squeo E A, *Int J Mod Manuf Technol*, 2(1) (2010).

12 Esat V, Darendeliler H & Gökler M I, *Mater Des*, 23 (2002) 223-229.

13 Hama T, Nagata T, Teodosiu C, Makinouchi A & Takuda H, *Int J Mech Sci*, 50 (2008) 175-192.

14 Alfaidi M F & Li X, *Ann Dunărea Jos Univ Galaţi, Technol Machine Build*, 27(32) (2009) 129-134.

15 Nicoara D, Teodorescu M & Ciocan D, *Romanian Pat*, RO-96746-B1.

16 eta/Dynaform 59, *Use'r Manual*, Version 5.9, http://www.eta.com.

17 Sharad G & Nandedkar V M, *IOSR J Mech Civil Eng*, 4 (2013) 53-56

18 Minh N Q, *Appl Mech Mater*, 703 (2014) 182-186.

19 Biradar A & Deshpande M D, *Int J Sci Res*, 3 (2014) 852-858.

20 Jiang W, Yang B, Guan X & Luo Y, *Acta Metall Sin* (Engl Lett), 26(3) (2013) 241-246.

21 Anggono A D, Siswanto W A, Omar B, *Res J Appl Sci, Eng Technol*, 4(14) (2012) 2036-2045.

22 Belytschko T, Liu W K & Moran B, *Finite Elements for Nonlinear Continua and Structures*, (Wiley, New York), 1996.

23 http://www.dynasupport.com/tutorial/contact-modeling-in-ls-dyna/contact-types